Electronic Supplementary Material (ESI) for New Journal of Chemistry.

Nitrogen-Rich Triphenylamine-based Porous Organic Polyaminal for The Adsorption/Separation of C1-C3 Light Hydrocarbons and Efficient Iodine Capture

Qiuyue Liu[§a], Lingmei Jiang [*§a, b], Jianhua Liu [c], Luhong Wei [c], Jian Zhang [a], Kuanyu Yuan[*]

[*] Corresponding author: Kuanyu Yuan (kylm02010810@aliyun.com) and Lingmei Jiang (jianglingmei@dlut.edu.cn)

[§] Qiuyue Liu and Lingmei Jiang contributed equally to this work.

[a] School of Chemistry, Chemical Engineering and Materials, Jining University, Qufu 273155, People's Republic of China

[b] Department of Polymer Materials and Engineering, Dalian University of Technology, Dalian 116024, People's Republic of China

[c] Shandong Pengrun New Materials Co.Itd, Jiaxiang 272400, People's Republic of China

1. Instrumentation and methods

Fourier-transformed infrared (FT-IR) spectra were characterized using a Bruker TENSOR-27 infrared spectrophotometer from 4000 cm^{-1} to 400 cm^{-1} at a resolution of 4 cm^{-1}. The sample was prepared using a conventional KBr disk method. ^{1}H NMR spectra were measured on a Brucker spectrometer using tetramethylsilane (TMS) as an internal standard at 400 MHz. Solid-state ^{13}C CP/MAS NMR was recorded on a Bruker AVANCE500 NMR spectrometer operating under a magnetic field strength of 9.4 T. The ^{13}C chemical shifts were referenced externally via the resonance of tetramethylsilane (TMS) of 0 ppm. Elemental analysis was conducted using an Elementarvario EL III elemental analyzer. Thermal gravimetric analysis (TGA) was performed on a Mettler-Toledo model SDTA -854 TG A system under a N_2 atmosphere at a heating rate of 10 ^{o}C min^{-1} from room temperature to 800 ^{o}C. Wide-angle X-ray diffraction (WAXD) images were collected on a Riguku D/MAX 2550 diffractometer under Cu-K_{α} radiation, at 40 kV and 200 mA, with a 2 θ range of 5-80^{o} (scanning rate of 10^{o} min^{-1}) at room temperature. The UV-vis adsorption spectra of dye solutions were obtained by a TU-1901 spectrophotometer at room temperature. N_2 sorption isotherm measurements were characterized at Quantachrome Quadrasorb apparatus with a Micromeritics surface area and pore-size analyzer. Before measurement, the samples were degassed for 12 h at 150 ^{o}C. Nonlocal density functional theory (NL-DFT) pore-size distributions (PSDs) were determined by using the carbon/slit-cylindrical pore mode of the Quadrawin software.

Gas Adsorption and Separation Performance

The CH_4, C_2H_6, C_3H_8, and CO_2 adsorption capacities of the synthesized polymers were evaluated according to adsorption isotherms collected at temperatures of 273 and 298 K over a pressure ranging from 0 to 1 bar. The calculated adsorption selectivities of C_3H_8/CH_4, C_2H_6/CH_4, C_3H_8/C_2H_6, C_2H_6/CO_2, C_3H_8/CO_2, and CO_2/CH_4 were based on the initial slope approach at 273 K and 298 K.

Iodine Vapor Adsorption Study

The iodine vapor capture experiment was carried out according the following procedure. Two small weighing bottles were separately charged with activated TPOA-F (10.0 mg) and TPOA-OH (10.0 mg). Then the bottles were placed in a sealed glass container equipped with excess iodine pellets at the bottom. The container was heated at 348 K under ambient pressure. Thereafter, the samples were cooled down to room temperature and weighed at different time intervals. The iodine uptakes of samples were calculated by weight gain according to:

$$\alpha = [(m_2 - m_1)/m_1] \times 100 \text{ wt \%}$$

where α is the iodine uptake, m_1 and m_2 are the mass of sample before and after adsorption of iodine. The iodine capture experiments were repeated three times to ensure the data was authentic and dependable. Meanwhile, the repetition adsorptions process were conducted to ensure the authenticity and dependence of the data. The performance of iodine adsorption in organic solution of polymer was also proceed. The 10.00 mg activated samples were added into the prearranged 300 mg/L iodine/n-hexane (5ml) and the absorbancy of the supernatant at different time were employed by UV-vis.

Iodine release came into being when the iodine-loaded samples (2.0 mg) were immersed in ethanol (10.0 mL) at room temperature. The iodine release behavior was monitored by the UV-vis absorbance of the iodine including ethanol within the monitored time frame.

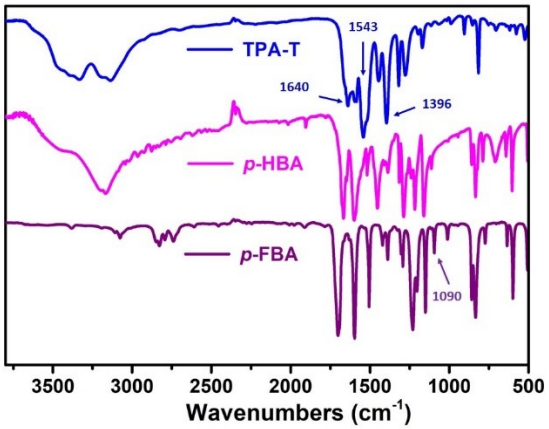

Figure S1. FT-IR spectra of the used monomer TPA-T, *p*-HBA and *p*-FBA.

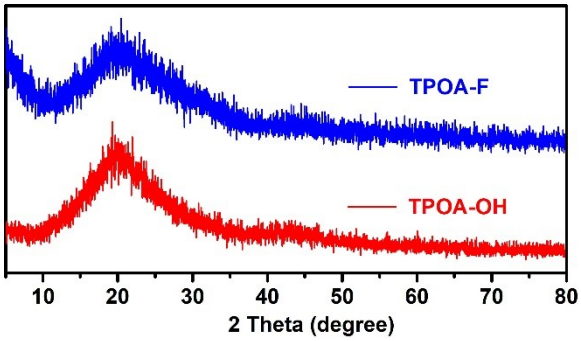

Figure S2. WAXD patterns of the TPOA-F and TPOA-OH.

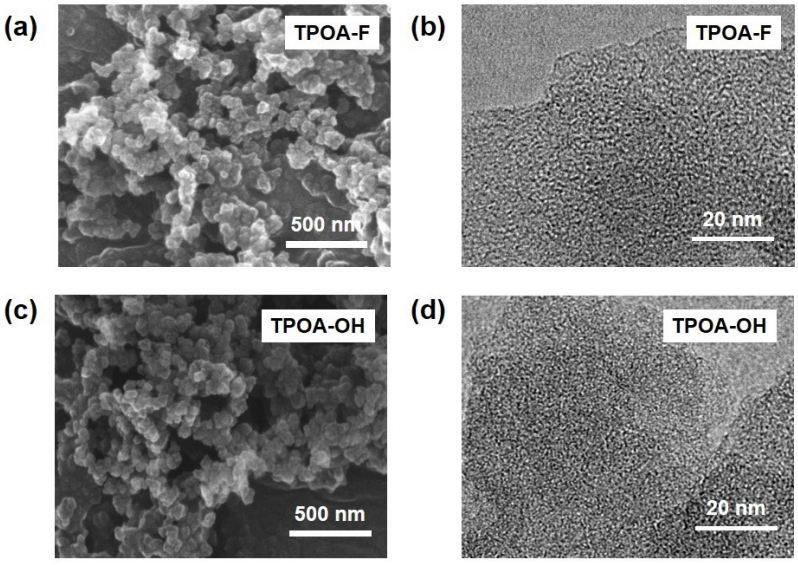

Figure S3. The SEM images for TPOA-F (a) and TPOA-F (c); The TEM images for TPOA-OH (b) and TPOA-OH (d).

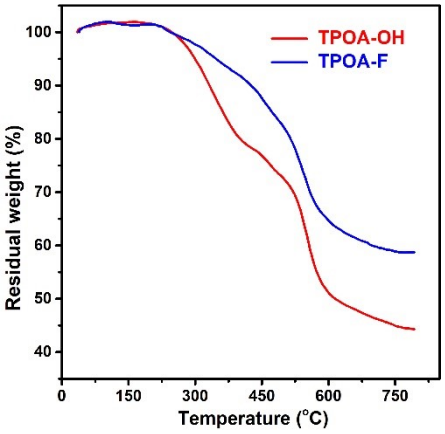

Figure S4. TGA traces of these two TPOAs under nitrogen atmosphere.

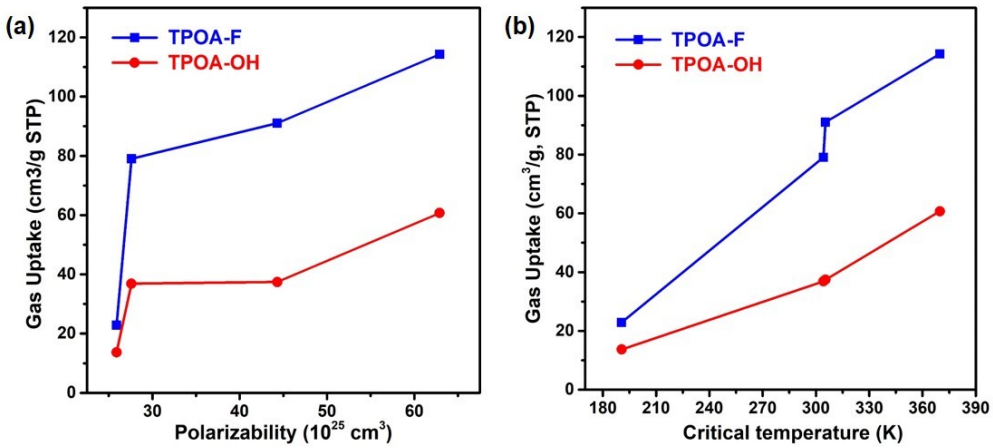

Figure S5. Dependencies of the uptake of C_3H_8, C_2H_6, CO_2, and CH_4 on their polarizabilities (a) and critical temperatures (b) in these two polymers.

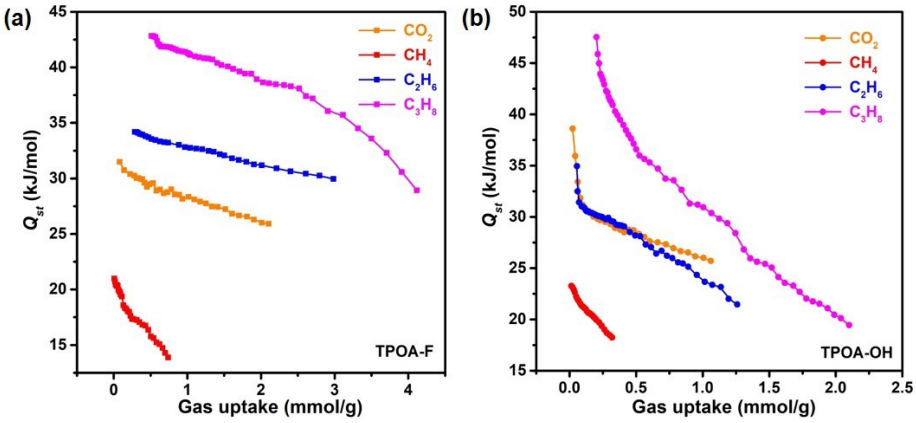

Figure S6. Variation of the adsorption enthalpies for C_3H_8, C_2H_6, CO_2, and CH_4 with the adsorbed amount in TPOA-F and TPOA-OH.

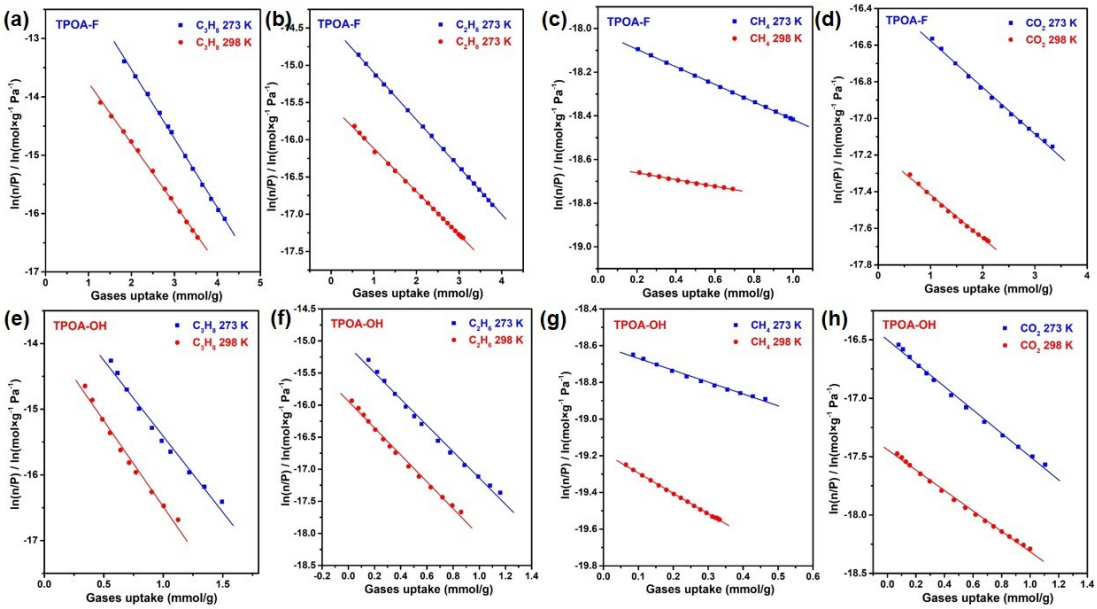

Figure S7. Virial plots of C_3H_8 (a), C_2H_6 (b), CH_4 (c), and CO_2 (d) for TPOA-F and C_3H_8 (e), C_2H_6 (f), CH_4 (g), and CO_2 (h) for TPOA-OH.

Table S1. Q_0, K_H and A_0 values for adsorption of CH_4, CO_2, C_2H_6, and C_3H_8 gases

Polymers	Gases	T (K)	K_H (mol g^{-1} Pa^{-1})	A_0 ln (mol g^{-1} Pa^{-1})	Q_0 (kJ mol^{-1})
TPOA-F	C_3H_8	273	1.421×10^{-5}	-11.161	39.6
		298	2.994×10^{-6}	-12.719	
	C_2H_6	273	5.244×10^{-7}	-14.461	34.2
		298	1.790×10^{-7}	-15.536	
	CH_4	273	1.501×10^{-8}	-18.015	28.5
		298	8.110×10^{-9}	-18.630	
	CO_2	273	8.161×10^{-8}	-16.321	29.6
		298	3.459×10^{-8}	-17.180	
TPOA-OH	C_3H_8	273	2.042×10^{-6}	-13.101	36.2
		298	9.501×10^{-7}	-13.867	
	C_2H_6	273	2.818×10^{-7}	-15.082	33.6
		298	1.200×10^{-7}	-15.938	
	CH_4	273	8.314×10^{-9}	-18.605	25.6
		298	4.663×10^{-9}	-19.184	
	CO_2	273	6.819×10^{-8}	-16.501	27.2
		298	2.665×10^{-8}	-17.440	

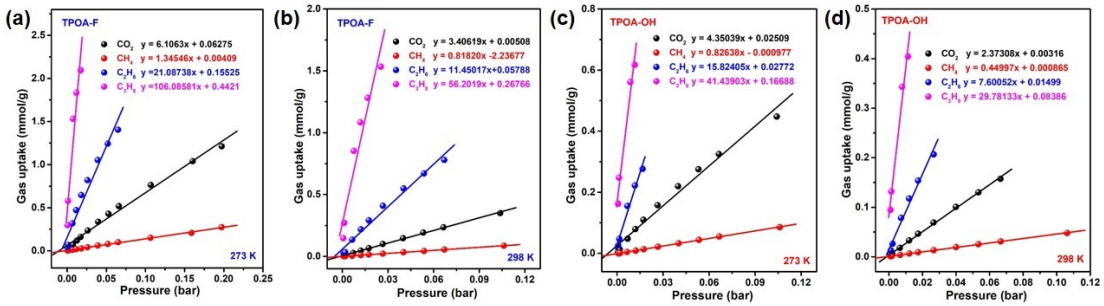

Figure S8. Adsorption selectivity of C_3H_8, C_2H_6, CH_4, and CO_2 for TPOA-F at 273 K (a) and 298 K (b) and TPOA-OH at 273 K (c) and 298 K (d).

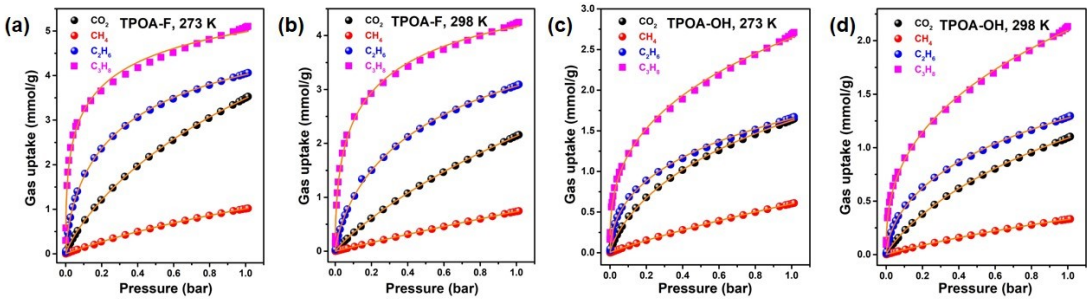

Figure S9. Experimental adsorption isotherms for C_3H_8, C_2H_6, CH_4, and CO_2, and their single-site Langmuir-Freundlich simulated curves (solid line) for TPOA-F at 273 K (a) and 298 K (b) & TPOA-OH at 273 K (c) and 298 K (d)

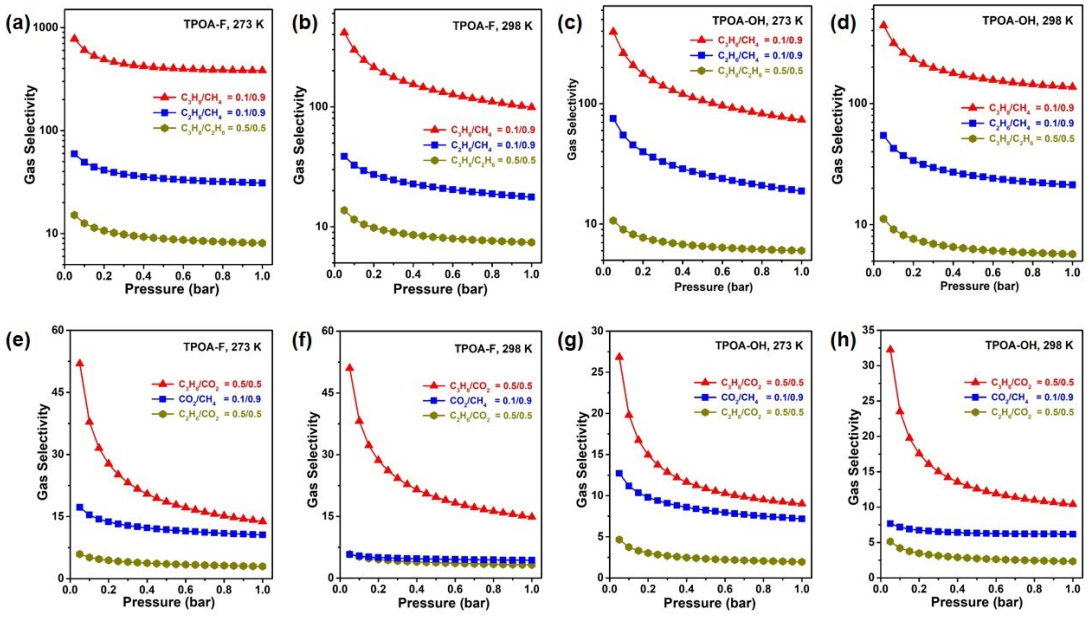

Figure S10. The IAST calculations for the adsorption selectivity of C_2H_6/CH_4, C_3H_8/CH_4, and C_3H_8/C_2H_6 & C_3H_8/CO_2, C_2H_6/CO_2, and CO_2/CH_4 for TPOAs at 273 K (a) and 298 K (b).

Table S2. Summary of iodine vapor uptake abilities of various porous adsorbents

Adsorbents	Temperature	Pressure	S_{BET}	Iodine uptake	Ref.

	(K)			(wt %)	
TPOA-F	358	1 bar	11179	234	**This work**
TPOA-OH	358	1 bar	565	343	**This work**
PAPOA-N(CH_3)$_2$.	358	1 bar	1444	356	Chem. Eng. J. (2022)
PHPOA-N(CH_3)$_2$	358	1 bar	972	272	137119-137128.
NAPOP-1	298	1 bar	657	206	J Polym Sci, Part A: Polym Chem. 2016;54(12):1724-30.
NAPOP-2	298	1 bar	458	239	
NAPOP-3	298	1 bar	702	241	
NAPOP-4	298	1 bar	626	265	
NRPP-1	353	1 bar	1579	192	ACS Appl Mater Interfaces. 2018;10(18):16049-58.
NRPP-2	353	1 bar	1028	222	
MALP-1	350	1 bar	1179	209	Ind. Eng. Chem. Res. 2019;58(37):17369-79.
MALP-2	350	1 bar	1126	219	
MALP-3	350	1 bar	1141	187	
MALP-4	350	1 bar	1093	203	
PAOP-1	353	1 bar	306	28	Journal of Applied Polymer Science, 2021, 138(12): 50054.
PAOP-2	353	1 bar	533	79	
PAOP-3	353	1 bar	367	49	
PAOP-4	353	1 bar	210	101	
TALPOP	353	1 bar	401	314	Scientific Reports. 2020;10(1):15943.
NRAPOP-1	350	1 bar	544	281	Journal of Materials Science. 2020;55(24):10896-909.
NRAPOP-2	350	1 bar	424	271	
PAN-B	348	1 bar	1254	317	Polymer. 2020:122401.
PAN-T	348	1 bar	1273	311	
PAN1	348	1 bar	616	133	J Appl Polym Sci. 2018;135(15):46106.
PAN2	348	1 bar	542	245	
PAN3	348	1 bar	194	281	
PAN4	348	1 bar	522	237	
PAN5	348	1 bar	439	189	
PAN-FPP5	348	1 bar	788	222	Ind. Eng. Chem. Res. 2020, 59, 7, 3269–3278
PAN-TPDA	348	1 bar	752	145	
Ag@Zeolite	368	1 bar	-	27.5	J. Am. Chem.Soc. 132 (2010) 8897-8899.
ZIF-8	350	1 bar	1630	125	J. Am. Chem.Soc. 133 (2011) 12398-12401.
NiMoS	333	1 bar	490	225	Chem. Mater. 27 (2015) 2619-2626.
PAF-1	298	40 Pa	5600	186	J. Mater. Chem. A 2 (2014) 7179-7187.
PAF-24	348	40 Pa	136	276	Angew. Chem. Int. Ed. 54 (2015) 12733-12737.

HCMP-1	358	1 bar	430	159	Macromolecules 49 (2016) 6322-6333.
HCMP-2	358	1 bar	153	281	Macromolecules 49 (2016) 6322-6333.
MOF-808	353	1 bar	2126	218	ACS Appl. Mater. Interfaces 12 (2020) 20429-20439.
NU-1000	353	1 bar	1930	145	ACS Appl. Mater. Interfaces 12 (2020) 20429-20439.
BTT-TAPT-COF	348	1 bar	545	276	Microporous Mesoporous Mater. 296 (2020) 109990
CMP-LS7	353	1 bar	507	277	J Hazard. Mater. 387 (2020) 121949.
CMP-LS8	353	1 bar	2028	529	J Hazard. Mater. 387 (2020) 121949.
TBTT-CMP@1	350	1 bar	58.84	442	Polym. Chem. 11 (2020) 2786-2790
TBTT-CMP@2	350	1 bar	64.23	357	Polym. Chem. 11 (2020) 2786-2790
TBTT-CMP@3	350	1 bar	62.98	352	Polym. Chem. 11 (2020) 2786-2790
CTF-Cl-1	350	1 bar	516	269	Chem. Asian. J, 2019, 14(19): 3259-3263.
CTF-Cl-2	350	1 bar	599	289	Chem. Asian. J, 2019, 14(19): 3259-3263.
CTF-Cl-3	350	1 bar	590	285	Chem. Asian. J, 2019, 14(19): 3259-3263.
CTF-Cl-4	350	1 bar	889	312	Chem. Asian. J, 2019, 14(19): 3259-3263.
S-HCP	348	1 bar	612.83	360	Sep. Purif. Technol. 228 (2019) 115739
CSU-CPOPs-1	348	1 bar	1032.4	494	ACS Appl. Mater. Interfaces 11 (2019) 27335-27342
CSU-CPOPs-2	348	1 bar	532.8	424	ACS Appl. Mater. Interfaces 11 (2019) 27335-27342
CSU-CPOPs-3	348	1 bar	268.8	347	ACS Appl. Mater. Interfaces 11 (2019) 27335-27342
TPB-DMTP COF	350	1 bar	1927	626	Adv. Mater. 2018, 30 (29), 1801991

TTA-TTB COF	350	1 bar	1733	495	Adv. Mater. 2018, 30 (29), 1801991
P-DPDA	348	1 bar	24.2	408	Microporous Mesoporous Mater. 2021;310:110596
P-TPB	348	1 bar	646.6	335	Microporous Mesoporous Mater. 2021;310:110596
P-PC	348	1 bar	540.4	268	Microporous Mesoporous Mater. 2021;310:110596

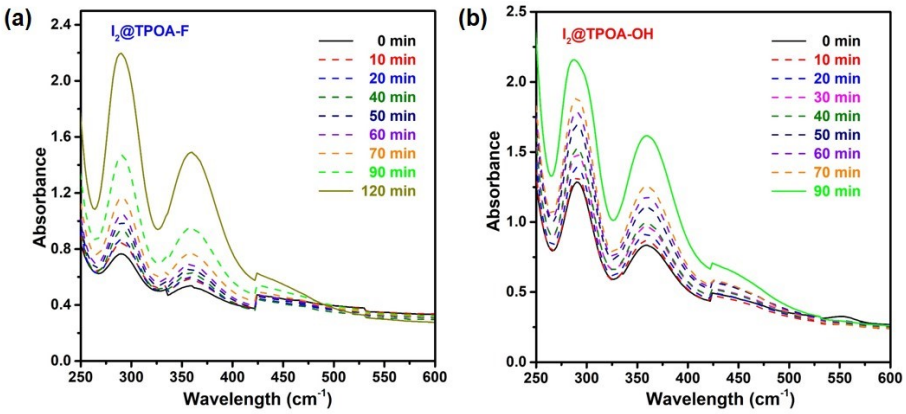

Figure S11. The UV-vis spectra of iodine released from I_2@TPOA-F (2 mg) in 10 mL of ethanol (a) and I_2@ TPOA-OH (2 mg) in 10 mL of ethanol (b)

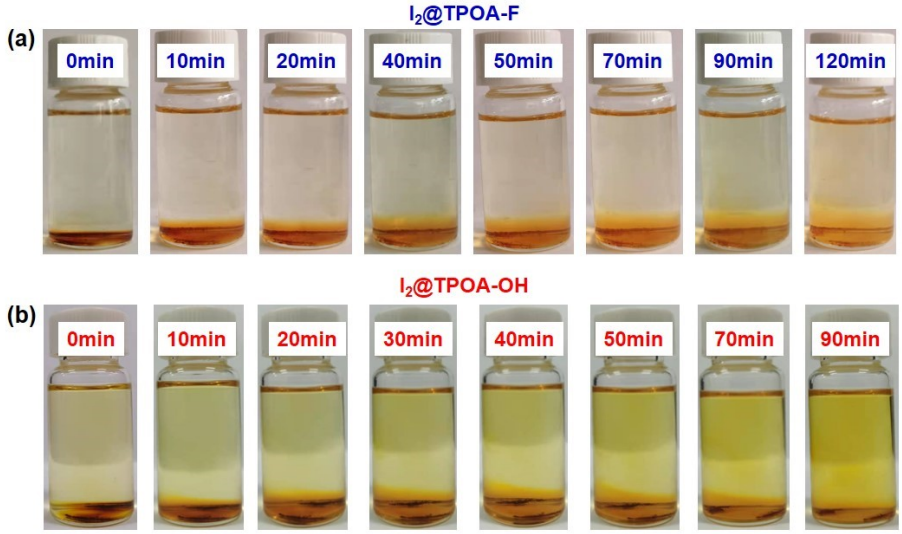

Figure S12. The UV-vis spectra of iodine released from I_2@TPOA-F (a) and I_2@ TPOA-OH (b)

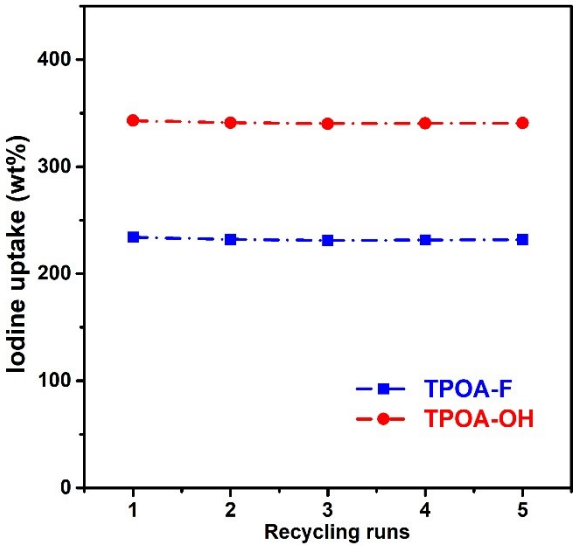

Figure S13. Recycle iodine capture experiments for these two TPOAs

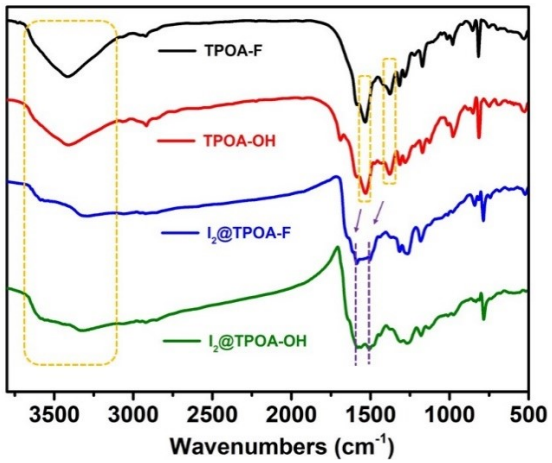

Figure S14. FT-IR spectra of TPOA-F, TPOA-OH, I_2@TPOA-F and I_2@TPOA-OH.

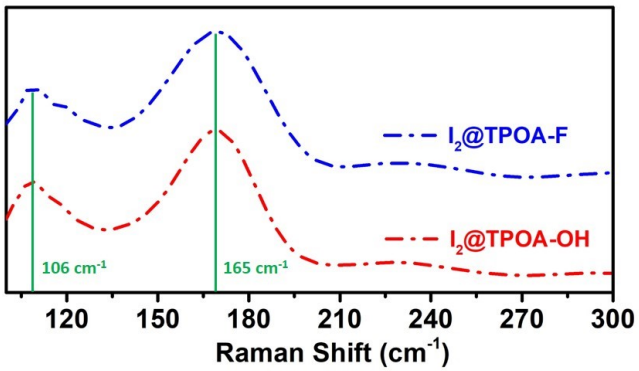

Figure S15. Their Raman spectra for the iodine-loaded TPOAs (I_2@ TPOAs).

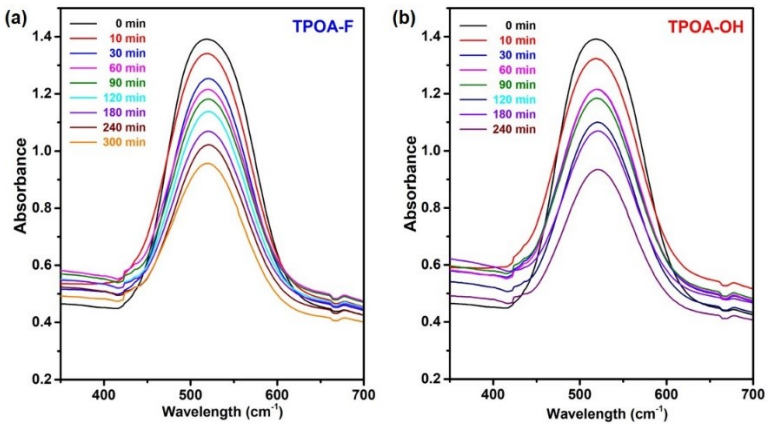

Figure S16. The removal of evolution of UV-Vis spectra of iodine adsorption in cyclohexane.

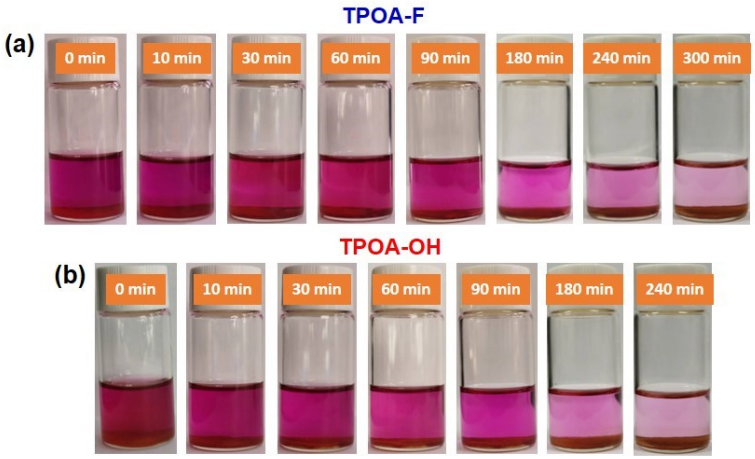

Figure S17. The photographs of iodine solution adsorption process of TPOA-F (a) and TPOA-OH (b).

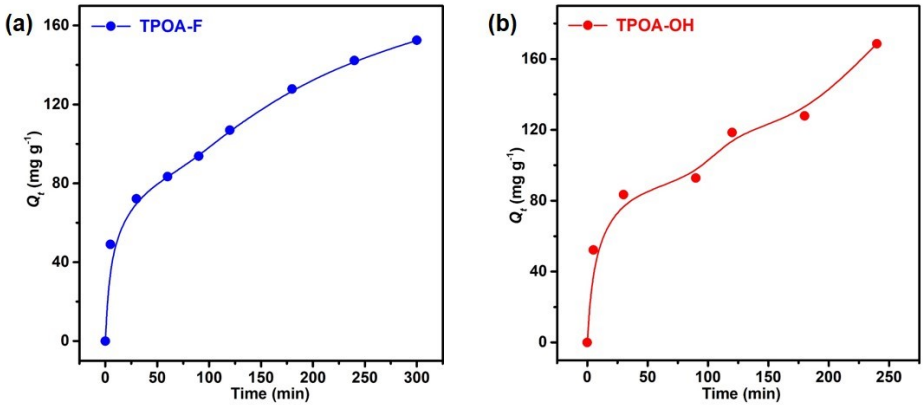

Figure S18. Adsorption kinetic of iodine on TPOAs.